Lab on a Chip

Cite this: *Lab Chip*, 2011, **11**, 3356

www.rsc.org/loc

TECHNICAL NOTE

Microfluidic baker's transformation device for three-dimensional rapid mixing†

Takao Yasui,*[ab] Yusuke Omoto,‡[c] Keiko Osato,[ab] Noritada Kaji,§[ab] Norikazu Suzuki,[c] Toyohiro Naito,[ab] Masaki Watanabe,[ab] Yukihiro Okamoto,[ab] Manabu Tokeshi,[ab] Eiji Shamoto[c] and Yoshinobu Baba[abd]

Received 22nd April 2011, Accepted 19th July 2011
DOI: 10.1039/c1lc20342h

We developed a new passive-type micromixer based on the baker's transformation and realized a fast mixing of a protein solution, which has lower diffusion constant. The baker's transformation is an ideal mixing method, but there is no report on the microfluidic baker's transformation (MBT), since it is required to fabricate the complicated three-dimensional (3D) structure to realize the MBT device. In this note, we successfully fabricate the MBT device by using precision diamond cutting of an oxygen-free copper substrate for the mould fabrication and PDMS replication. The MBT device with 10.4 mm mixing length enables us to achieve complete mixing of a FITC solution ($D = 2.6 \times 10^{-10}$ m^2 s^{-1}) within 51 ms and an IgG solution ($D = 4.6 \times 10^{-11}$ m^2 s^{-1}) within 306 ms. Its mixing speed is 70-fold higher for a FITC solution and 900-fold higher for an IgG solution than the mixing speed by the microchannel without MBT structures. The Péclet number to attain complete mixing in the MBT device is estimated to be 6.9×10^4.

Introduction

In the past decades microfluidic systems have been widely used in chemistry, biology, and nanobiotechnology, including DNA[1] or protein analysis,[2] cell sorting,[3] and chemical reactions.[4] Mixing inside microchannels plays an important role in those microfluidic analysis systems, and many researchers have made efforts to develop innovative mixing techniques inside microchannels.[5] In particular, mixing of solutes with a low diffusion coefficient inside microchannels is important and useful for a variety of applications including immunoassay,[6] and it is desirable to get the most efficient and rapid mixing possible inside them.

Due to the low Reynolds number (*Re*) inside microchannels, mixing of fluids there is a challenging task. Several passive-type micromixers have been developed.[7–10] Most passive-type mixers depend on simple mixing techniques without any external power sources, unlike active-type mixers, which use sources such as ultrasonic,[11] magnetic stirring,[12] and bubble induced acoustic actuation.[13] In the passive-type mixers, only the structural design induces the mixing of fluids which is affected by the convection flow and large interface of fluids. Therefore the efficiency of mixing depends on the structural design which is best fabricated by a simple and smart process; examples include serpentine structures,[7] bas-relief structures on the bottom of the microchannels,[8] Tesla structures,[9] and split and recombine structures.[10] 3D serpentine structures were designed to cause chaotic advection, however, relatively high *Re* is required to achieve it.[7] Bas-relief structures on the bottom of the microchannels, referred to as a staggered herringbone mixer, and alternating herringbone patterns which exchange the positions of the centres of 3D helical flow caused chaotic mixing.[8] Transverse dispersion with modified Tesla structures, using the Coanda effect, has been demonstrated over a wide range of flow rates.[9] Split and recombine structures include two general chaotic mixing mechanisms of "lamination" by the successive alignment of F-shape mixing structures in two layers and "advection" by the whole 3D serpentine channel structures.[10] These structures, however, are not enough to achieve all the desired features of an ideal micromixer, *e.g.* providing rapid mixing, high mixing efficiency, a wide range of flow rates, and being suited to mass production (*i.e.* having disposability), because of the limitation for fabrication methods based on a two-dimensional (2D) patterning process which makes a complicated design quite a difficult task to demonstrate.

[a]*Department of Applied Chemistry, Graduate School of Engineering, Nagoya University, Furo-cho, Chikusa-ku, Nagoya, 464-8603, Japan*
[b]*FIRST Research Center for Innovative Nanobiodevices, Nagoya University, Furo-cho, Chikusa-ku, Nagoya, 464-8603, Japan. E-mail: yasui.takao@e.mbox.nagoya-u.ac.jp; Fax: +81 52 7894666; Tel: +81 52 7893560*
[c]*Department of Mechanical Science & Engineering, Graduate School of Engineering, Nagoya University, Furo-cho, Chikusa-ku, Nagoya, 464-8603, Japan*
[d]*Health Research Institute, National Institute of Advanced Industrial Science and Technology (AIST), Hayashi-cho 2217-14, Takamatsu, 761-0395, Japan*

† Electronic supplementary information (ESI) available: Samples, confocal microscopy, details of cross-sectional views, experimental details, SEM images, no mixer results, simulations, and movies. See DOI: 10.1039/c1lc20342h

‡ Current address: Denso Corporation, Showa-cho 1-1, Kariya 448-8661, Japan.
§ Current address: Graduate School of Science, ERATO Higashiyama Live-Holonics Project, Nagoya University, Japan.

In this paper, we propose a new design for the 3D micromixer, which is based on the baker's transformation. The baker's transformation, which is also called a Smale horseshoe map, provides the highest mixing performance as demonstrated in chaotic theories[14] (see also the ESI†, Fig. S1). A device based on the baker's transformation is an ideal choice to use for mixing of fluids, but its extremely difficult fabrication has prevented researchers from applying it to micromixers. Herein, we have fabricated baker's transformation structures with isovolumetric change (keeping a constant volume) on an oxygen-free copper block by using precision diamond cutting.[15] We quantitatively studied its mixing performance to attain complete mixing over a wide range of flow rates. The mixing performance of the MBT device is evaluated using FITC (fluorescein isothiocyanate; diffusion coefficient: 2.6×10^{-10} m^2 s^{-1})[16] and goat anti-mouse IgG (immunoglobulin G; diffusion coefficient: 4.6×10^{-11} m^2 s^{-1})[17] dissolved in phosphate buffered saline (PBS). To the best of our knowledge, this is the first successful demonstration of the baker's transformation structure for a micromixer.

Fabrication

The basic machining process of the mould for the MBT device was planing, which is one of cutting processes. We used an ultraprecision planing machine, NIC-300 (Nagase Integrex Co., Ltd.), which consists of three feed tables with double hydrostatic oil guide ways on the *XYZ* axes, two rotary index tables on the *BC* axes and a five-axis control system. The top surface of the mould was finished with a custom-ordered ultraprecision diamond cutting tool (A.L.M.T. Diamond Corp.), which has a 1 mm nose radius. Then, the proposed microchannels were machined with another ultraprecision diamond tool (A.L.M.T. Diamond Corp.), which has a straight cutting edge of 20 μm width. An optical surface profiler, NewView 6200 (Zygo Corp.), was applied to measure the 3D configuration (Fig. S2, ESI†).

Results and discussion

1. Baker's transformation

In the simplest baker's transformation case, we stretch and cut a square, and then fuse and fold the pieces as indicated in Fig. S1†. The proposed MBT device has successive 3D configuration changes to realize folding, stretching, cutting, and fusing of microfluids. Fig. 1(a) illustrates the MBT mixing process. Two types of fluids are indicated by two colours, blue and yellow. The successive 3D configuration changes fold the blue fluid onto the yellow fluid gradually. After completing the folding, the combined fluids are stretched and then half of the fluids are bent 90°, which these steps make a great difference between baker's transformation and parallel lamination. The bent part of the fluids are cut or moved to the opposite side. Then the moved part is gradually folded onto the original fluids again, *i.e.* they are fused.

These steps (fold, stretch, cut, and fuse) make stacks of fluids. In order to confirm the desired baker's transformation has taken place, the microfluidic distribution of vertical cross-sectional views was investigated numerically. The numerical simulation results (ANSYS-CFX, ESI†) are displayed as cross-sectional views in the flow direction in Fig. 1(b). Although we did not expect that both edges of the fluids would be fully stacked, we could confirm that most were. Therefore, we can say our MBT design is valid for shortening the diffusion length.

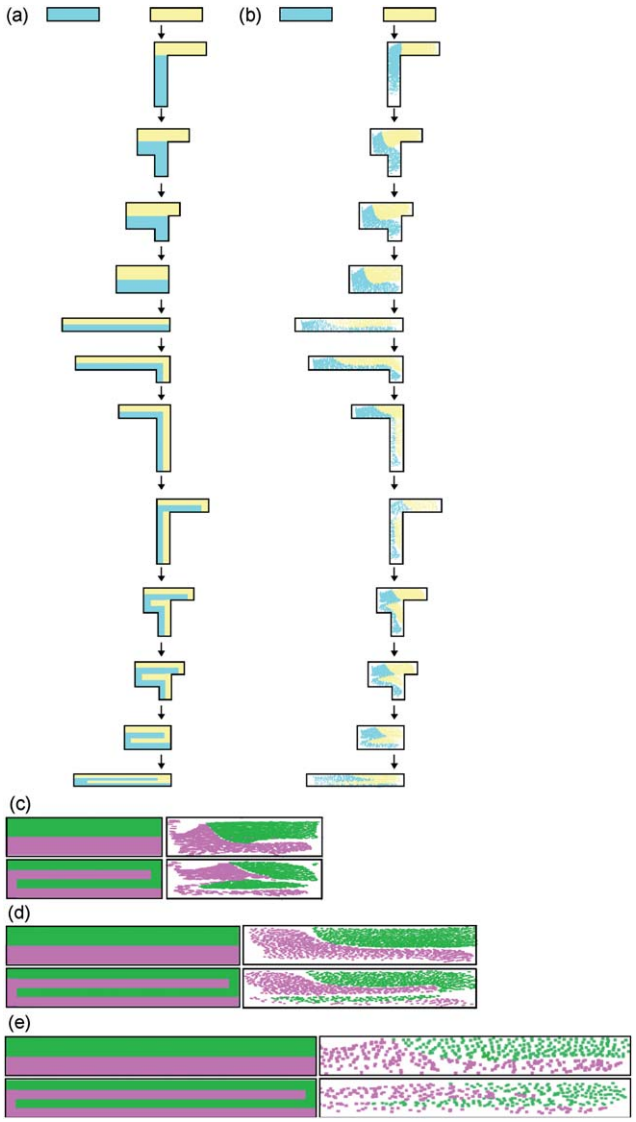

Fig. 1 Schematics of (a) mixing process of MBT device, (b) microfluidic distributions derived from numerical simulations for the MBT device, and (c)–(e) ideal mixing process and microfluidic distributions derived from numerical simulations in aspect ratios of (c) 4, (d) 6, and (e) 8. Each image shows the cross-sections in the most stretched channel. One MBT process was performed from the top views to bottom ones.

An aspect ratio of microchannel is a considerable factor for mixing efficiency because it affects the design of microchannel and ease of fabrication. The aspect ratio used here means the ratio of channel depth to channel width in the most stretched channel. In the left images of Fig. 1(c)–(e), we revealed an ideal MBT in the most stretched channel with the aspect ratio of 4, 6 and 8, respectively, and one MBT process was performed beginning at the top images. As was expected, the higher aspect ratio showed the larger contact area of fluids, the aspect ratio of 8 could realize most ideal MBT in these images.

The right images of Fig. 1(c)–(e) represented the microfluidic distributions derived from numerical simulation results in the most

stretched channel. MBT processes were performed beginning at the top images in the aspect ratios of (c) 4, (d) 6, and (e) 8. As shown in these figures, the aspect ratio of 8 showed the larger contact area of fluids than other aspect ratios, and therefore, one MBT process with large aspect ratio enabled us to mix fluids more efficiently.

Another considerable factor is the difficulty of the fabrication. Due to the difficulty of the fabrication, 20 μm was the minimum limitation for depth in our technique. And also we had the working area limitation for width in our technique up to 160 μm. Although it will be possible to fabricate in the working area over 160 μm, there was a trade-off between mixing efficiency and fabrication. Taking the Péclet number into consideration, the smaller size of channel dimensions and the faster flow velocities are required. From the above reasons, we selected the channel with the aspect ratio of 8 (160 μm × 20 μm, width and height, respectively).

2. MBT devices

Based on the numerical simulation, mixing performance, and ease of fabrication (Fig. 1), we fabricated the MBT device as shown in Fig. 2. The number of the cycles of baker's transformation structures, including folding, stretching, cutting, and fusing of microfluids, plays an important role in mixing solutions because it leads directly to the number of stacked layers. A schematic of the mould is shown in Fig. 2(a). On an oxygen-free copper block (30 × 60 mm), the MBT device is designed to have two inlets, injection microchannels with 10 mm length and 20 μm height, 10.4 mm length MBT structures, and an outlet channel with 33 mm length and 20 μm height.

The 3D configuration of the structures is shown in Fig. 2(b), and a rotation animation of the structures is provided in Movie S1 (ESI†) for further understanding. These structures were designed to have transverse (x–y) and longitudinal (x–z) movements of solutions at the same time to realize the MBT like that of Fig. 1. Vertical cross-sections of the MBT device along the y axis are illustrated in Fig. 2(c). The dotted lines indicate the replication point in Fig. 2(b). One cycle of the MBT device is 1040 μm and there are 10 cycles in all. The MBT device has the constant cross-section of channel at an arbitrary position as shown in Fig. 2(c) leading to keeping a constant volume inside the channel at an arbitrary position, and therefore, the back pressure of the device is as the same as a simple straight channel.

To get a better understanding of the MBT structures, a series of replication process was illustrated in Fig. 2(d)–(f). Fig. 2(d) and

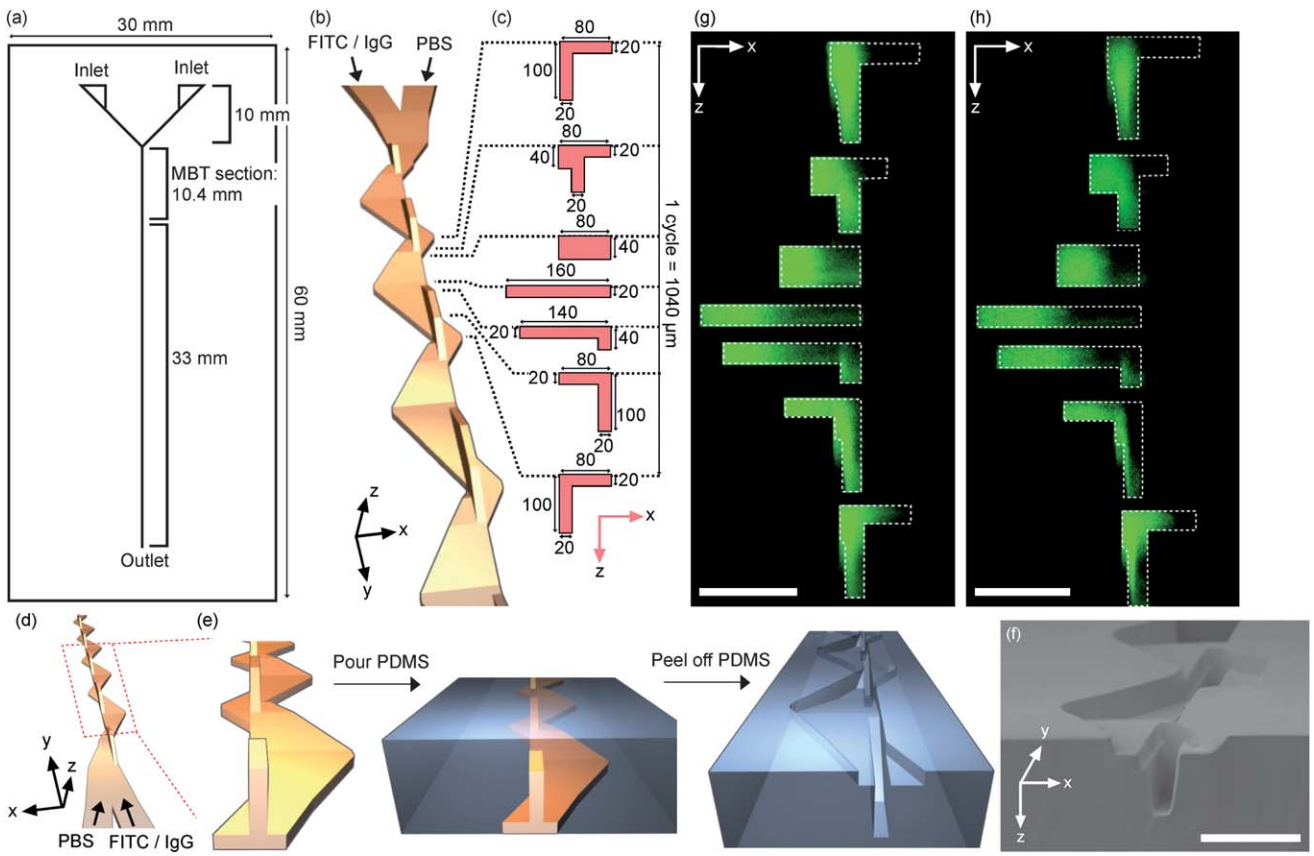

Fig. 2 (a) Schematic of the MBT device. It consists of two inlets, injection channels, mixing section, and outlet channels. (b) Schematic 3D diagram of the mould for the MBT device. (c) Schematic illustrations of vertical cross-sections of the MBT device. Numbers show the dimensions as μm. One cycle of the MBT structures is 1040 μm. The dotted lines indicate the replication points in the mould. (d) Schematic 3D diagram of the mould, (e) detail of the boxed area in (d), pouring the PDMS image, and peeling off the PDMS image. (f) SEM image of the MBT device taken by the S-4300 (Hitachi). A vertical cross-sectional view of the MBT device. The scale bar is 100 μm. (g) and (h) Series of confocal micrographs for one cycle in a microchannel such as in (c). Flow rate was 100 mm s^{-1}. The scale bar is 100 μm and the white dotted lines indicate channel outlines. (g) The mixing of FITC solution and PBS. (h) The mixing of IgG solution and PBS.

the left one of Fig. 2(e) showed the mould of MBT structures and the magnified image in boxed area, respectively. By pouring poly (dimethylsiloxane) (PDMS) onto the mould (the middle one of Fig. 2(e)), curing and cutting the PDMS, the MBT device is fabricated from the mould (the right one of Fig. 2(e)). SEM image of the MBT device is given as a cross-sectional view (Fig. 2(f)).

The flames in Fig. 2(g) and (h) show confocal micrographs of the vertical cross-sections of a channel similar to those in Fig. 2(c) for one cycle; the mixing of FITC solution and PBS (Fig. 2(g)) and the mixing of IgG solution and PBS (Fig. 2(h)). The movies (ESI† Movies S2 and S3) show the process of mixing of FITC solution and PBS or IgG solution and PBS in the MBT device. The solutions had two-directional movements, transverse and longitudinal.

3. Mixing performance

To evaluate the mixing performance, the mixing ratio was calculated using the following formula;[18]

$$\left(1-\sqrt{\frac{1}{N}\sum_{i=1}^{N}\left(I_i-I_i^{\text{perf.mix}}\right)^2\Big/\frac{1}{N}\sum_{i=1}^{N}\left(I_i^0-I_i^{\text{perf.mix}}\right)^2}\right)\times 100 \quad (1)$$

where N, I_i, I_i^0, and $I_i^{\text{perf.mix}}$ are the total number of pixels, the fluorescence intensity at pixel i, the fluorescence intensity at pixel i without mixing or diffusion, and the fluorescence intensity of the completely mixed solution at pixel i, respectively. Generally, the 90% mixing ratio was regarded as complete mixing.[8]

The mixing ratios of FITC solution *vs.* PBS and IgG solution *vs.* PBS are shown in Fig. 3(a) and (b), respectively. The mixing ratio was calculated using Formula (1). The MBT device provided complete mixing of FITC solution and PBS at flow velocities up to 400 mm s^{-1} for 10 cycles, and complete mixing of IgG solution and PBS was attained at velocities up to 50 mm s^{-1} for 10 cycles; these were characterized by the values of low Reynolds number ($Re = Ul/\nu < 100$, where U is the average flow velocity, l is the typical cross-sectional dimension, and ν is the kinematic viscosity of the fluid). The difference in maximum flow rate to attain complete mixing between FITC (400 mm s^{-1}) and IgG solution (50 mm s^{-1}) was attributed to the different diffusion coefficients. From these figures, we saw the mixing performance increased as the number of cycles increased, *e.g.* when mixing IgG solution and PBS at 4 mm s^{-1} flow velocity, the mixing ratios were 44, 72, and 97% after 1, 5 and 10 cycles, respectively.

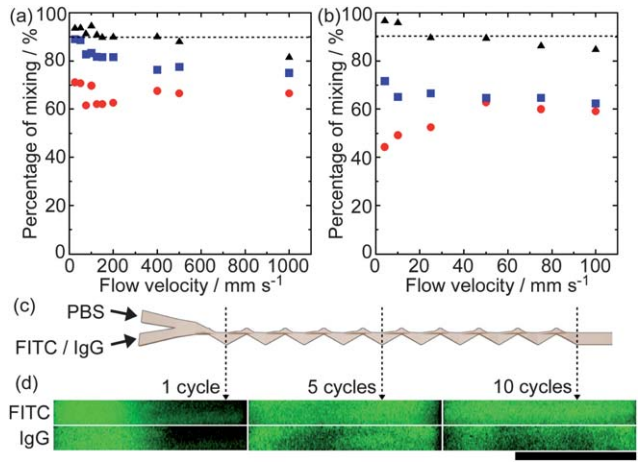

Fig. 3 (a) Mixing ratio of FITC solution and PBS *vs.* flow rate. (b) Mixing ratio of IgG solution and PBS *vs.* flow rate. Circles, squares, and triangles show $\Delta y = 1.04$, 5.02, and 10.4 mm (*i.e.* after 1, 5, and 10 cycles of mixing), respectively. The dotted line indicates 90% mixing ratio. (c) Schematic diagrams of the MBT device as in Fig. 2(c). (d) Confocal micrographs of vertical cross-sections of a microchannel such as in Fig. 2 (c) at different cycles. Flow rate was 100 mm s^{-1}. The scale bar is 100 μm. The upper ones are the mixing of FITC solution and PBS. The lower ones are the mixing of IgG solution and PBS.

Fig. 3(d) shows confocal micrographs of the vertical cross-sections of the most stretched channel (160 μm × 20 μm, width and height, respectively) for different cycles as indicated in Fig. 3 (c). In these micrographs, FITC solution and PBS in the upper part of Fig. 3(d) or IgG solution and PBS in the lower part of Fig. 3(d) were introduced to observe the mixing behaviour inside the MBT device; a syringe pump operated at a constant flow velocity of 100 mm s^{-1} was used. As the simulation results indicated, the right edge of the channel was not fully mixed for both FITC and IgG after 5 cycles. At this flow velocity, FITC solution and PBS were completely mixed after 10 cycles, but IgG solution and PBS were not. This insufficient mixing comes from the 10-fold smaller diffusion coefficient of IgG compared to FITC. Comparison of these results with those for the microchannel without MBT structures (Fig. S3, ESI†) showed that the mixing performance was dramatically increased by the MBT device.

To determine the residence time to attain complete mixing, we calculated the time to achieve complete mixing from Fig. 3(a) and (b) by dividing the length by flow velocity. Fig. 4(a) shows the mixing ratio *vs.* residence time after 10 cycles with the MBT device. For comparison, the mixing ratio *vs.* residence time in the microchannel without MBT structures is also shown. The logarithmic fitting curves are expressed based on experimental points. We could calculate the residence time to attain complete mixing from these fitting curves. The residence time for FITC in the MBT device was 51 ms and for IgG 306 ms. Considering the

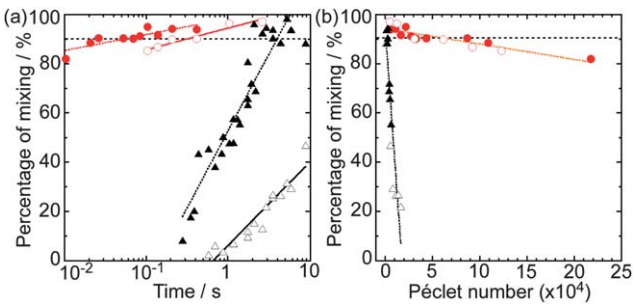

Fig. 4 The mixing ratio *vs.* (a) residence time and (b) Péclet number in the MBT device (circles) and microchannel without MBT structures (triangles). Filled and open symbols show FITC and IgG mixing, respectively. The dotted line indicates 90% mixing ratio. (a) The logarithmic fitting curves are expressed as $Y = 98.35 + 6.49\log X$ (red filled circles), $Y = 94.50 + 8.74\log X$ (red open circles), $Y = 52.59 + 62.71\log X$ (black filled triangles), and $Y = 6.12 + 34.12\log X$ (black open triangles); where Y is the percentage of mixing and X is the residence time. (b) The linear fittings are expressed as $Y = 94.31–6.25 \times 10^{-5}X$ (10.4 mm mixing length in MBT device) and $Y = 94.07–5.32 \times 10^{-3}X$ (35 mm mixing length in a microchannel without MBT structures); where Y is the percentage of mixing and X is the Péclet number.

Table 1 Typical parameters of passive-type micromixers

Type	Channel width × height/μm	Channel length/mm s^{-1}	Velocity to attain perfect mixing/mm s^{-1}	Maximum mixing rate	Pe	Materials	Ref.
MBT	160 × 20	10.4	4–400	97%	$1.0–6.9 \times 10^4$	PDMS	This work
3D Serpentine	300 × 150	18	150–445	97%	$1.6–4.7 \times 10^4$	Silicon-glass	7
Herringbone	200 × 70	2–30	10–3000	≥90%	$2000–9.0 \times 105$[a]	PDMS	8
2D/Tesla	200 × 90	7	69	88%	—[b]	COC[c]	9
Split and recombine	250 × 60	10	11	90%	5200	COC	10

[a] The Péclet number in 10.4 mm mixing length was $Pe = 4.9 \times 10^4$. [b] Because it could not achieve the perfect mixing (>90%). [c] COC = Cyclic olefin copolymer.

residence times in the microchannel without MBT structures of 4.0 s for FITC and 297 s for IgG (that could not be attained in this mixing length but was calculated from the fitting curve), our MBT device showed significant potential for mixing FITC solution and IgG solution more efficiently and rapidly in a 10.4 mm mixing length microchannel than in a microchannel without MBT structures, and mixing rate was more than 70-fold faster for FITC solution and 900-fold faster for IgG solution.

To characterize the mixing efficiency, we also used the Péclet number ($Pe = Ul/D$, where D is the molecular diffusion coefficient). Fig. 4(b) shows the mixing ratio *vs.* the Péclet number in a 10.4 mm mixing length of MBT device and 35 mm mixing length of the microchannel without MBT structures. The linear fittings are expressed based on experimental points. Comparison of the Péclet number to attain complete mixing in the MBT device ($Pe = 6.9\times10^4$) with that in the microchannel without MBT structures ($Pe = 7.7\times10^2$) showed our MBT device had a higher mixing efficiency despite in a shorter mixing length.

To compare our MBT device with other passive-type micromixers in terms of several parameters, we summarized channel dimensions, velocity to attain perfect mixing, maximum mixing rate, the Péclet number, and materials (Table 1). And moreover our MBT device even showed a little more efficient mixing performance than that in Bas-relief structures ($Pe = 4.9 \times 10^4$)[8] in this 10.4 mm mixing length.

Conclusions

A novel passive micromixer, termed a microfluidic baker's transformation (MBT) device, was proposed for rapid mixing in a microchannel. The mixing mechanism was based on the baker's transformation as a chaotic mixer and complete mixing of FITC solution and IgG solution was achieved in respective residence times of 51 and 306 ms for a 10.4 mm mixing length microchannel. The Péclet number to attain complete mixing in a 10.4 mm mixing length of the MBT device was 6.9×10^4. Moreover our MBT device showed high mixing efficiency over a wide range of flow rates and mass-produced PDMS replication from the mould with keeping a constant volume. Because we fabricated 3D structures for MBT by the ultraprecision planing in a single mould, we can easily integrate our MBT channel and other microfluidic components into a whole lab-on-a-chip device. We also laminate our MBT device into other microchannel due to PDMS replication. The remaining difficulty to be overcome is the fabrication time, but the optimized MBT structures would get rid of that difficulty. Once the most appropriate mould for MBT structures is determined, we can easily mix protein solutions, which generally have a low diffusion coefficient, inside a microchannel. Furthermore, the MBT structures can be more improved by shortening the length of the cycles and increasing the number of cycles. We expect the MBT structures will provide benefits for most microfluidic devices.

Acknowledgements

This research is partially supported by the Japan Society for the Promotion of Science (JSPS) through its "Funding Program for World-Leading Innovative R&D on Science and Technology (FIRST Program)", the Grant-in-Aid for Scientific Research (B), the Grant-in-Aid for JSPS Fellows, and Global COE Program for Education and Research of Micro-Nano Mechatronics, MEXT, Japan.

Notes and references

1 M. A. Burns, B. N. Johnson, S. N. Brahmasandra, K. Handique, J. R. Webster, M. Krishnan, T. S. Sammarco, P. M. Man, D. Jones, D. Heldsinger, C. H. Mastrangelo and D. T. Burke, *Science*, 1998, **282**, 484–487.
2 M. Ikami, A. Kawakami, M. Kakuta, Y. Okamoto, N. Kaji, M. Tokeshi and Y. Baba, *Lab Chip*, 2010, **10**, 3335–3340.
3 K. Ozaki, H. Sugino, Y. Shirasaki, T. Aoki, T. Arakawa, T. Funatsu and S. Shoji, *Sens. Actuators, B*, 2010, **150**, 449–455.
4 M. W. Losey, M. A. Schmidt and K. F. Jensen, *Ind. Eng. Chem. Res.*, 2001, **40**, 2555–2562.
5 N.-T. Nguyen, *Micromixers; Fundamentals, Design and Fabrication*, William Andrew Inc., Norwich, NY, 2008.
6 T. Tachi, N. Kaji, M. Tokeshi and Y. Baba, *Lab Chip*, 2009, **9**, 966–971.
7 R. H. Liu, M. A. Stremler, K. V. Sharp, M. G. Olsen, J. G. Santiago, R. J. Adrian, H. Aref and D. J. Beebe, *J. Microelectromech. Syst.*, 2000, **9**, 190–197.
8 A. D. Stroock, S. K. Dertinger, A. Ajdari, I. Mezic, H. A. Stone and G. M. Whitesides, *Science*, 2002, **295**, 647–651.
9 C. C. Hong, J. W. Choi and C. H. Ahn, *Lab Chip*, 2004, **4**, 109–113.
10 D. S. Kim, S. H. Lee, T. H. Kwon and C. H. Ahn, *Lab Chip*, 2005, **5**, 739–747.
11 Z. Yang, H. Goto, M. Matsumoto and R. Maeda, *Electrophoresis*, 2000, **21**, 116–119.
12 L. H. Lu, K. S. Ryu and C. Liu, *J. Microelectromech. Syst.*, 2002, **11**, 462–469.
13 R. H. Liu, J. Yang, M. Z. Pindera, M. Athavale and P. Grodzinski, *Lab Chip*, 2002, **2**, 151–157.
14 J. M. Ottino, *The kinematics of Mixing: Stretching, Chaos, and Transport*, Cambridge University Press, Cambridge, 1989.
15 M. J. Madou, *Fundamentals of Microfabrication: the Science of Miniaturization*, CRC Press, Boca Raton, Florida, 2002.
16 N. Periasamy and A. S. Verkman, *Biophys. J.*, 1998, **75**, 557–567.
17 D. de Beer, P. Stoodley and Z. Lewandowski, *Biotechnol. Bioeng.*, 1997, **53**, 151–158.
18 T. J. Johnson, D. Ross and L. E. Locascio, *Anal. Chem.*, 2002, **74**, 45–51.

